Biomass Conversion and Biorefinery
https://doi.org/10.1007/s13399-022-03200-x

ORIGINAL ARTICLE

Scale-Up of production of 5-hydroxymethylfurfural-rich adhesive precursors and structural features of humin side products

Wilfried Sailer-Kronlachner[1,2] · Catherine Rosenfeld[1,2] · Stefan Böhmdorfer[3] · Markus Bacher[3] · Johannes Konnerth[2] · Thomas Rosenau[3] · Antje Potthast[3] · Andreas Geyer[4] · Hendrikus W. G. van Herwijnen[1,2]

Received: 1 April 2022 / Revised: 25 July 2022 / Accepted: 8 August 2022

Abstract
A batch reaction system (volume 1 L) for scaled-up production of 5-HMF-based adhesive precursor solutions from industrially available fructose syrup was developed. The stabilizing effect of sodium dithionite addition was demonstrated. With this system, no concentration steps are needed in the production of adhesive precursors for wood composite board production. The reaction system was optimized in a design of experiment approach to achieve good reaction conditions and to produce reaction solutions with 5-HMF concentrations appropriate for adhesive synthesis. Only three runs in the adjusted system are required to produce enough precursor for the synthesis of 10 kg of adhesive, thereby enabling the testing of the adhesive systems in particle board trials.
Furthermore, the structure of humin side products from different reaction stages, formed from 5-HMF and byproducts by condensation, aldol-like reactions and attack on furan ring systems, was investigated. The data were compared to information from literature and possible elements of humin structures are proposed.

Keywords 5-Hydroxymethylfurfural (5-HMF) · Acidic dehydration · Scale-up · Adhesive precursor · Humin structure

1 Introduction

Today's wood board industry relies heavily on fossil-based binder systems that utilize formaldehyde as reactive component. The replacement of fossil-based binders with alternatives made from renewable resources is highly desired to reduce the environmental impact of the used systems. Taking particleboards as example, the adhesive accounts for approximately 10–14 wt% of their dry mass. A worldwide production of 95 million m^3 of particleboard per year [1], at a density of around 650 kg/m^3, requires approx. 6–9 megatons of adhesive annually. This shows that even replacing a part of this adhesive amount with renewable-based counterparts can have a major impact in terms of the sustainability of particleboard production. Furthermore, formaldehyde has been classified as cancerogenic by the European Union [2]. The utilization of carbohydrates, such as starch, celluloses and hemicelluloses, which make up 75% of the available biomass [3], is a desirable alternative for adhesive production. These carbohydrates could be converted into monosaccharides, such as glucose or fructose, and further to follow-up products to replace toxic or fossil-based chemicals.

5-Hydroxymethylfurfural (5-HMF) is considered an important bio-based platform chemical that displays potential in binder production as well as in various other fields. Examples are the production of polyesters or green solvents from 5-HMF secondary products, such as 2,5-furandicarboxylic acid (FDCA) [4]. FDCA can be produced by oxidation of 5-HMF [5] and is one popular example for the

✉ Wilfried Sailer-Kronlachner
w.sailer-kronlachner@wood-kplus.at; w.sailer@boku.ac.at

1 Kompetenzzentrum Holz GmbH - Wood K Plus, Altenberger Str.69, 4040 Linz, Austria

2 Department of Material Science and Process Engineering, Institute of Wood Technology and Renewable Materials, University of Natural Resources and Life Sciences, Vienna, Konrad-Lorenz Str. 24, 3430 Tulln, Austria

3 Department of Chemistry, Institute of Chemistry of Renewable Resources, University of Natural Resources and Life Sciences, Vienna, Konrad Lorenz-Straße 24/I, 3430 Tulln, Austria

4 FRITZ EGGER GmbH & Co. OG Holzwerkstoffe, Tiroler Straße 16, 3105 Unterradlberg, Austria

Published online: 17 August 2022

variety of possible applications starting from 5-HMF and its derivatives. The utilization of 5-HMF as cross-linker in adhesive systems is a promising approach in the development of sustainable products that could replace the currently used fossil-based adhesive systems in the wood panel industry. 5-HMF has several reaction sites that are interesting for cross-linking: the aldehyde moiety, the alcohol group and the furanic ring system. The research interest in 5-HMF is high and a lot of work has been invested in studies on its production and utilization, as evident from the rise in the number of publications on the topic (Fig. 1).

Although 5-HMF is seen as a very potent and versatile platform chemical, no large-scale production has been established up to now. Only a small-scale (up to 300 t/a) commercial plant is operated by AVA Biochem in Switzerland. As a consequence, large-scale industrial availability of 5-HMF is not yet given [6]. This makes in situ approaches that use 5-HMF as reactant without isolation or purification very interesting.

Good overviews of methods in 5-HMF production and the involved solvents, catalytic systems and reaction mechanisms, are available in the literature as follows. Van Putten et al. covered dehydration chemistry aspects from various sources as well as process chemistry and process technology. The review also considers nutritional and toxicological topics and provides information on the multiple possible applications of 5-HMF [7]. Yu et al. focused in their review on catalytic systems and underlying mechanisms [8], while Hu et al. addressed the catalytic and autocatalytic production of 5-HMF from biomass [9]. The challenging industrial production has recently been the topic of an account from our group [6], whereas Zhao et al. discussed the production of 5-HMF from lignocellulosic biomass in their review [10]. Slak et al. addressed process intensification and 5-HMF separation and purification [11] as well as a multiscale modeling approach for (hemi)cellulose hydrolysis and cascade hydrotreatment of 5-HMF [12].

In general, 5-HMF is produced from hexoses through acidic dehydration. One molecule of D-fructose generates one equivalent of 5-HMF and three equivalents of water (Scheme 1). Rehydration, elimination and ring opening from

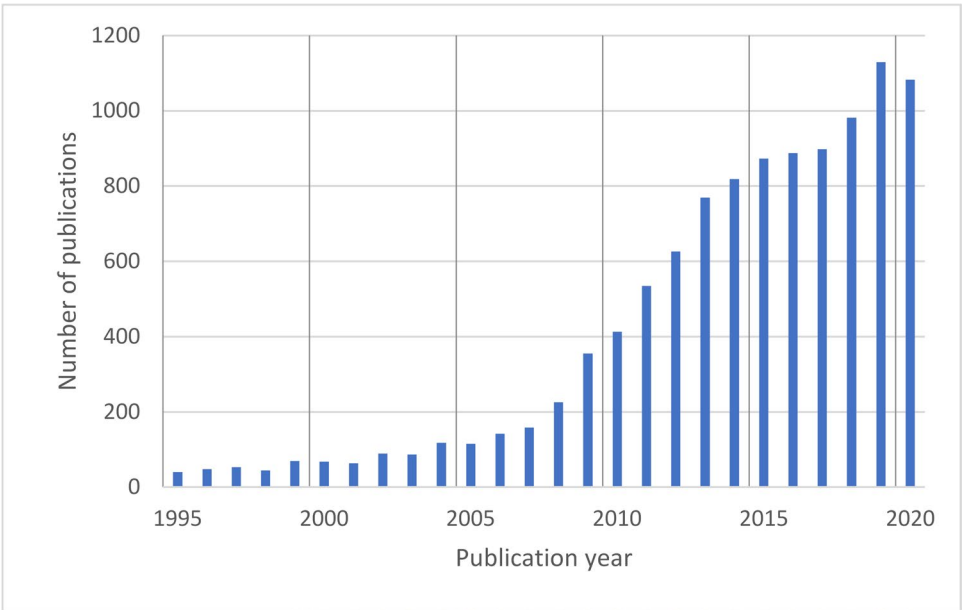

Fig. 1 Publications on 5-HMF per year, keyword search for "hydroxymethylfurfural" in CAS Scifinder (Oct 10, 2021)

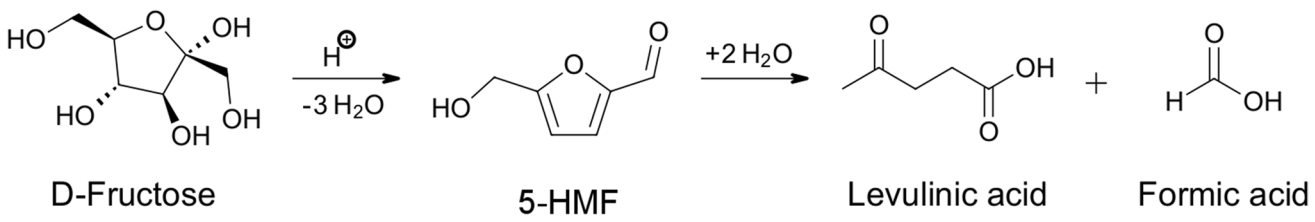

Scheme 1 Dehydration of fructose to 5-HMF and side reaction of 5-HMF to formic acid and levulinic acid

5-HMF might produce levulinic acid and formic acid in an important side reaction (Scheme 1).

In a previous publication [13], the successful production of 5-HMF-rich binder precursors in a continuous mesoreactor system from fructose solutions catalyzed by sulfuric acid was reported. This "adhesive precursor" is an aqueous compound mixture comprising non-reacted fructose, formed 5-HMF, the side products levulinic acid and formic acid as well as humins (5-HMF oligomers and condensation products). The publication also included detailed information on the choice of the catalyst as well as the solvent system. This setup achieved good 5-HMF yields of 49 mol%. There are obviously systems that achieve higher 5-HMF yields, but these systems use either organic solvents (biphasic systems) or heterogeneous catalysis, which would require additional separation steps. A drawback of this continuous system was its limitation to maximum fructose concentrations of 15 wt% in the reaction solutions. This was due to clogging issues at higher fructose concentrations. The produced solutions had thus to be concentrated by vacuum distillation to achieve 5-HMF concentrations of ~ 60 g/L (~ 5 wt%) and to allow the production of final precursors for binders with high solid contents. The continuous setup was chosen for the precise reaction and temperature control [14], which were problematic in batch reaction systems. Inconsistent heating and cooling times lead to irreproducible results. In this work, we tested the hypothesis that the improvement of a batch reaction system with a pressurized dosing system and a fast cooling system would eliminate these effects and enable the use of high sugar concentrations of 60 wt% in the starting solution. The important question was whether a carbohydrate-based precursor containing the same levels of 5-HMF as the precursor produced with the continuous reaction system can be obtained with the improved batch reaction system, thereby eliminating the concentration step that was necessary before.

Another important part of this work was to scale the reaction to a size that enables the production of adhesive amounts needed for the manufacture of laboratory particleboards. To produce a laboratory board of 50 × 50 cm with a thickness of 16 mm, approximately 400 g of adhesive are needed (10% resin content in the board). The goal was a system that allows the production of 10 kg of adhesive, an amount that allows production of several particle boards in one press series, in a reasonable time. At a flow rate of 7 ml/min and with the need of the concentration of the produced solution, this has not been easily achievable in the continuous reaction system.

One major side reaction in the precursor production process is the formation of black, tarry side products, usually denoted as humins. The formation of these compounds led to the clogging issues in the continuous reaction system. Structural features of the humins produced in both 5-HMF production variants, continuous and batch, were investigated and compared to data available in the literature [15–19].

In renewable-based adhesive design, green chemistry principles are important since the developed system will be used to produce a sustainable binder system for wood composites. The goal of this work is the development of an in situ system for adhesive production that avoids the need for solvent recycling, as well as any energy consuming extraction or purification steps. This is achieved by the utilization of a homogeneous catalyst that can remain in the final adhesive system. With this, no additional waste streams are generated. The environmental impact of the whole adhesive system will be checked in a LCA analysis which is to be published on the project homepage [20].

Gomes et al. demonstrated the stabilization of 5-HMF during its production or distillation by the addition of sodium dithionite ($Na_2S_2O_4$) [21]. The hypothesis that the use of sodium dithionite during the precursor production in our batch reaction system would lead to similar stabilization effects and therefore could reduce humin side product formation was tested and the system was optimized in a design of experiment (DoE) approach.

2 Material and methods

Fructose, in the form of a syrup containing 70.5 wt% carbohydrates (consisting of 95% fructose and 5% of other mono, di- and trisaccharides), was supplied by Cargill Deutschland GmbH and diluted to the desired concentrations with deionized water. Sulfuric acid (H_2SO_4, 98% p.a.) and sodium dithionite ($Na_2S_2O_4$, EMPLURA®) were purchased from Sigma-Aldrich (Merck Supelco).

2.1 Experiments with increasing sugar concentrations

Producing the adhesive precursors in a conventional batch reaction system caused problems with regard to reproducibility due to difficulties with the temperature management. To reduce the problem with inconsistent heating and cooling times, a büchiglasuster® versoclave Typ 4E/1.0 L reactor (Büchi AG, Switzerland) with a pressurized dosing system was used. In a typical experiment, the fructose syrup, containing 70.5 wt% of sugar, was diluted to the target concentration with deionized H_2O and preheated to the reaction temperature. Diluted sulfuric acid catalyst, the appropriate amount to reach a final concentration of 1% in the reaction

solution, was added and the reaction time was started. The water used to dilute the acid was subtracted from the amount of solvent used to dilute the sugar syrup. Experiments with rising sugar content in the starting solution, from 10–60 wt%, at a constant reaction temperature of 120 °C were performed. The reaction time was 45 min with 15 min cooling time to below 100 °C. Batch size was 400 g or 700 g for most of the experiments (mass of the complete reaction solution including all reactands). In the case of the higher charge, the cooling time to reach a solution temperature below 100 °C was 17 min.

2.2 Modification of the batch reaction system

After the first set of experiments with rising sugar concentration, a cooling system was fitted to the reactor. This was done to achieve comparability of reactions at different reaction temperatures by eliminating large differences in cooling times. A system that allowed emptying of the pressurized reactor in a safe, quick and reproducible manner was developed. A metal coil cooled with cold water was fitted between the reactor and a pressure container. Pressure from the container was relieved through tubing into a washing vessel filled with water for gas washing and avoidance of air contamination and smell. The system enabled emptying of the reactor within 1 min, thereby cooling the reaction solution to 30–40 °C. Figure 2 shows the final reaction setup that was used in the subsequent design of experiment (DoE) optimization with sodium dithionite stabilization.

2.3 Design of experiment (DoE) optimization of the reaction system with sodium dithionite stabilization

For the DoE, a randomized two-level factorial design was chosen. Reaction time (15, 30, 45 min), reaction temperature (120, 130, 140 °C) and sodium dithionite content (0.1, 0.55, 1 wt% of the overall reaction mass) were the influencing factors, with the 5-HMF yield, the levulinic acid yield and the mass loss during reaction (the mass of humins produced) being the three monitored responses. The conditions for the DoE were chosen based on previous work [13]. All reactions were performed with a starting solution containing 60 wt% of carbohydrates, the final catalyst content in the reaction solution was set to 1%, and all experiments followed the same procedure:

The fructose solution was transferred into the reactor, batch size was 600 g with a stirring speed of 250 rpm in all DoE experiments. Concentrated sulfuric acid was diluted with 20 ml of deionized water and prepared for addition in the pressurized dosing system. The reactor was sealed and the reaction solution was heated to the desired reaction temperature. After stabilization of the reactors jacket temperature and the solution temperature, the sulfuric acid was added to the reaction solution to start the reaction. After the desired reaction time, the reactor was emptied into the pressure container through the cooling coil, which was cooled using an ice bath. The coil was emptied by blowing pressurized air through the system and the reactor was immediately

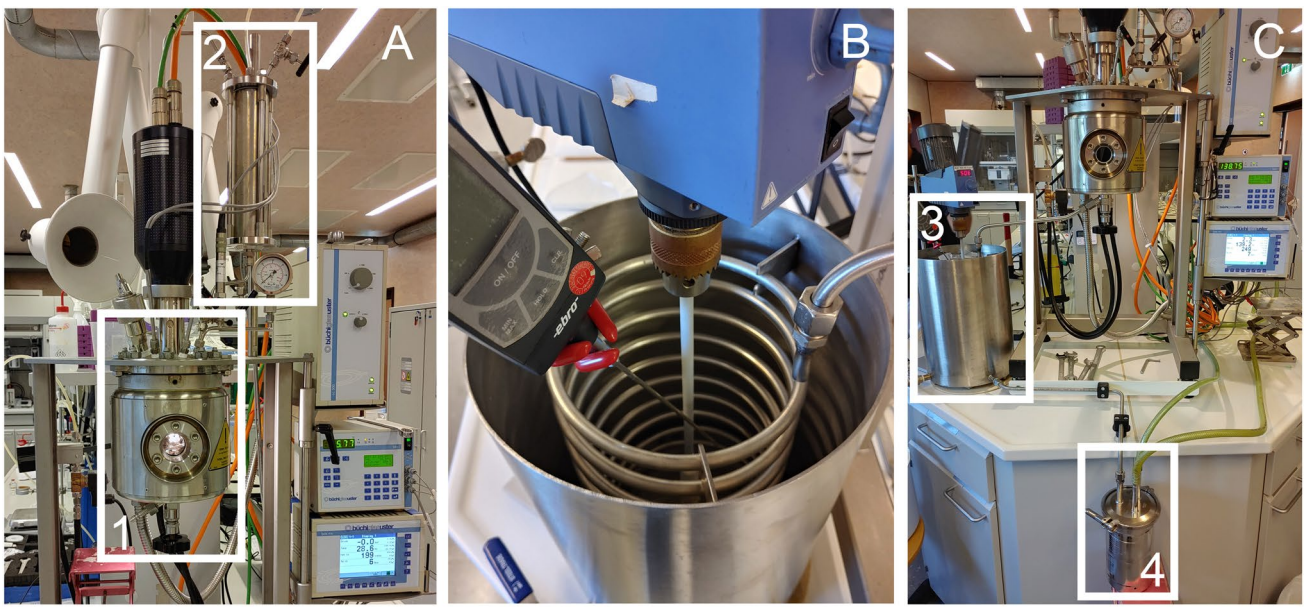

Fig. 2 **A**: Main reactor (1) with pressurized dosing system (2); **B**: cooling coil; **C**: reactor with installed cooling system (3) and pressure container (4)

filled with hot water to avoid charring of residues on the hot reactor walls.

2.4 Humin samples for analysis

Two different humin samples were taken. The first sample was obtained from the mesoreactor process described in our previous work [13]. During the concentration of the reaction solution to obtain the final precursor, a sticky black polymer was formed, which was collected and dried for further analysis. Freeze-drying was chosen as drying method to avoid further change of the sample. The second humin sample collected was produced during the batch reaction process described in this work. Black, charry polymer residues were collected from the surfaces of the reactor and the stirrer after the reaction solution had been removed and were freeze-dried for further analysis. An ALPHA 1–4 LDplus freeze-dryer (Martin Christ Gefriertrocknungsanlagen GmbH, Germany) with the condenser set to -55 °C and vacuum at 0.045 mbar was used. Figure 3 shows the appearance of humin samples taken and the deposition of humins on the stirrer of the batch reactor system.

2.5 Analytical methods

FTIR spectra were recorded on a FTIR Single-Range spectrometer in ATR mode (PerkinElmer Frontier, Waltham, MA, United States). A spectrum of air was recorded as background before each measurement. Each sample was analyzed in the range from 4000 cm^{-1} to 600 cm^{-1} with 8 scans per measurement and two measurements per sample. The measurements are presented as absorbance. The humin samples were freeze-dried for 48 h prior to analysis.

All reaction solutions were analyzed directly by ^{1}H NMR spectroscopy for determination of the 5-HMF concentration. All ^{1}H NMR spectra were acquired at room temperature on a Bruker Avance II 400 instrument (resonance frequency 400.13 MHz for ^{1}H) equipped with a 5 mm liquid N_2 cooled probe head (Prodigy) with z gradients. For the measurements, 500 µL of the sample solution was mixed with 30 µL of 0.34 mM NaOAc as the internal standard and 100 µL of D_2O (99.8% D, Eurisotop, Saint-Aubin, France). A relaxation delay of 2 s was used. Molar yields were calculated based on the initial fructose amount in the reaction solution. Weight percentages were based on the final concentration of 5-HMF and levulinic acid in the reaction solution.

Liquid NMR spectra were recorded on a Bruker Avance II 400 (resonance frequency 400.13 MHz for ^{1}H and 100.61 MHz for ^{13}C) equipped with a 5 mm N_2-cooled broadband observe cryoprobe head (Prodigy) with z gradients at room temperature with standard Bruker pulse programs. The samples were dissolved in 0.6 ml of DMSO-d_6 (99.8% D, Eurisotop, Saint-Aubin, France). Chemical shifts are given in ppm, referenced to the residual solvent signal (δ_H 2.49 ppm, δ_C 39.6 ppm). All two-dimensional experiments were performed with 1 k × 256 data points,

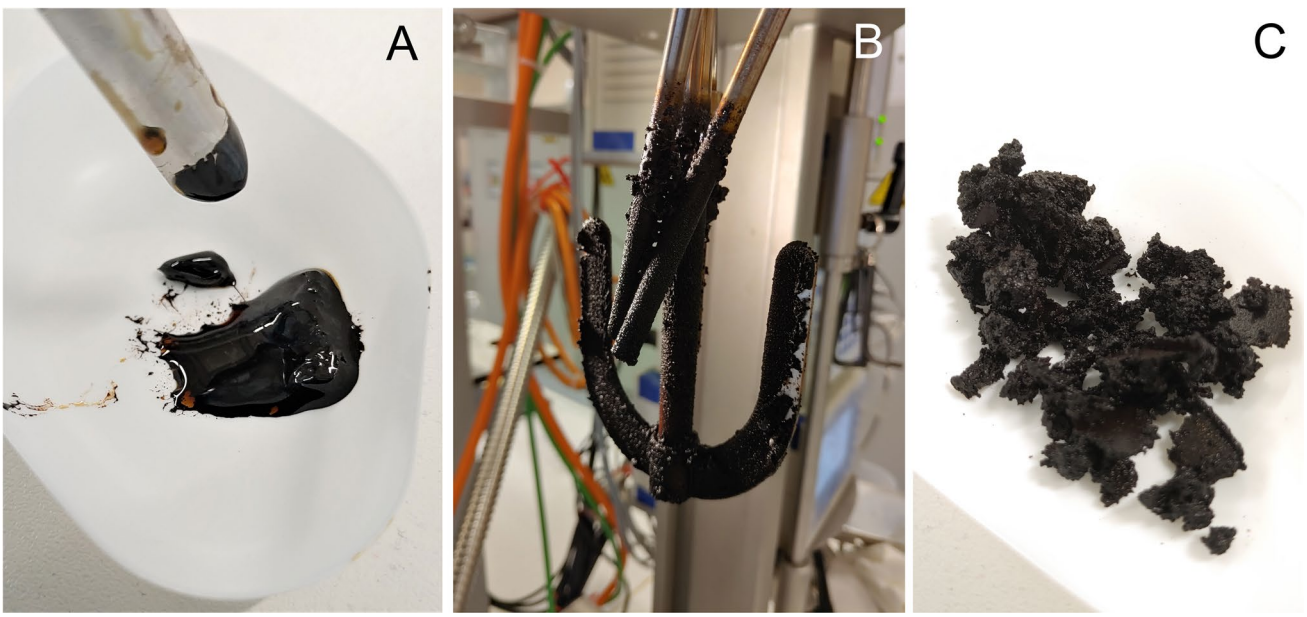

Fig. 3 **A**: Humin sample from the mesoreactor production process; **B**: Humin deposition on the stirrer of the batch reactor; **C**: humin sample from the batch process (without sodium dithionite stabilization)

while the number of transients and the sweep widths were optimized individually. HSQC experiments were acquired in edited mode using adiabatic pulse for inversion of ^{13}C and GARP-sequence for broadband ^{13}C-decoupling, optimized for $^{1}J_{(CH)} = 145$ Hz. An example of a typical ^{1}H NMR spectrum of the product mixture is given in the supporting information, including peak assignment.

Solid state NMR experiments were performed on a Bruker Avance III HD 400 spectrometer (resonance frequency of ^{1}H of 400.13 MHz and ^{13}C of 100.61 MHz, respectively), equipped with a 4 mm dual broadband CP-MAS probe. ^{13}C spectra were acquired by using the basic cross-polarization sequence at ambient temperature with a spinning rate of 12 kHz, a cross-polarization (CP) contact time of 2 ms, a recycle delay of 2 s, SPINAL-64 ^{1}H decoupling and an acquisition time of 50 ms. 3 k data points were sampled to give a spectral width of 300 ppm. Chemical shifts were referenced externally against the carbonyl signal of glycine with $\delta = 176.03$ ppm. The acquired FIDs were apodized with an exponential function (lb = 33 Hz) prior to Fourier transformation.

A Polyma 214 (Netzsch-Gerätebau GmbH, Germany) was used for the differential scanning calorimetry (DSC) measurements. Humin samples (2 – 5 mg) were measured in a closed, high-pressure steel crucible. The device was calibrated by measuring gallium, indium, tin and bismuth at a heating rate of 5 K/min. Typical measurements were taken from 20 °C to 350 °C. The data were analyzed with Netzsch Proteus® software (Netzsch-Gerätebau GmbH, Selb, Germany) and Origin 2016G software (OriginLab Corporation, Northampton, MA, USA).

3 Results and discussion

3.1 Experiments with increasing fructose concentrations

Experiments were conducted to determine whether the same 5-HMF levels (60 g/L) as previously produced in the continuous reaction system by concentration of the solution can be also achieved in the batch reactor by using high sugar concentrations from the beginning. Figure 4 shows the results of the experiments performed at 120 °C.

The 5-HMF yield of 73 g/L, obtained at 60 wt% of fructose in the starting solution, exceeded the targeted 60 g/L. This amount of 5-HMF proved to be sufficient to significantly improve adhesive properties and was therefore considered quite satisfactory [13, 22]. All experiments of this series (Fig. 4) were performed once, while the experiment at 40 wt% fructose concentration was repeated 4 times to test the reproducibility of the reaction results. Only minute deviations were found: 55.1 ± 0.6 g/L (variation of ± 1.1 mol%). These results confirm that the selected setup and pressurized dosing system enable high reproducibility, inconsistencies in heating time were successfully eliminated. While the absolute obtainable mass of 5-HMF improved with higher (starting) fructose concentration, the molar yield decreased from 20 to 13%. The reason for this is that the (starting) fructose concentration was increased while the catalyst concentration remained the same. Since also side product formation (see humin depositions in Fig. 3) increases at higher fructose concentrations, optimization of this system was required. This was

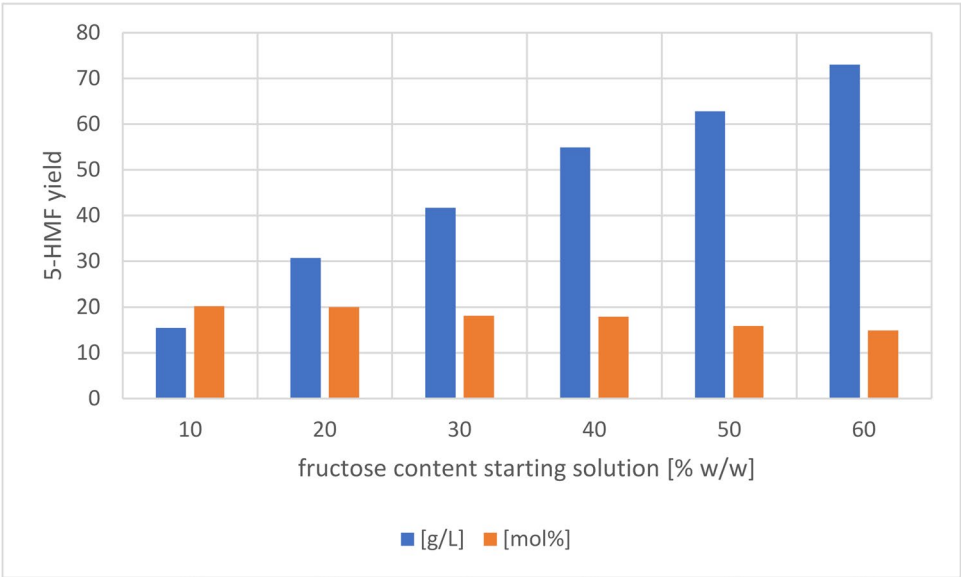

Fig. 4. 5-HMF yields from starting solutions with increasing amounts of fructose (n = 1)

also one reason for including the stabilization experiments with sodium dithionite in the DOE.

While the pressurized dosing system used in the investigation with different fructose starting concentrations allowed the precise setting of heating times, the difference in cooling times still rendered the comparison of reactions at different temperatures difficult. Cooling a batch reactor from 140 °C to < 100 °C takes significantly longer than cooling from, e.g., 120 °C. This results in a longer time at elevated reaction temperature after the desired reaction time, which leads to incomparable results, since the reaction temperature is no longer constant during the cooling process. Therefore, the above-mentioned cooling system (see 2.2.) was designed and installed. Experiments confirmed that efficient cooling to < 50 °C was achieved from all reaction temperatures up to 140 °C in under 1 min. Since the reaction rates of the dehydration reaction are very low below 100 °C, this was sufficient to make comparison of different reaction temperatures feasible.

3.2 Batch reaction optimization results (DoE)

The three main responses (to the factors reaction temperature, reaction time and sodium dithionite concentration) studied in the DoE setup were the 5-HMF yield, the levulinic acid yield and the yield loss during the reaction. The latter corresponds to the humin formation during the reactions and is based on the reasonable approximation that all side reactions of fructose not affording 5-HMF eventually lead to humins. Figure 5 depicts the influence of the three main factors on the 5-HMF yield. Of these influencing factors, the reaction temperature had the largest influence on the outcome, followed by the

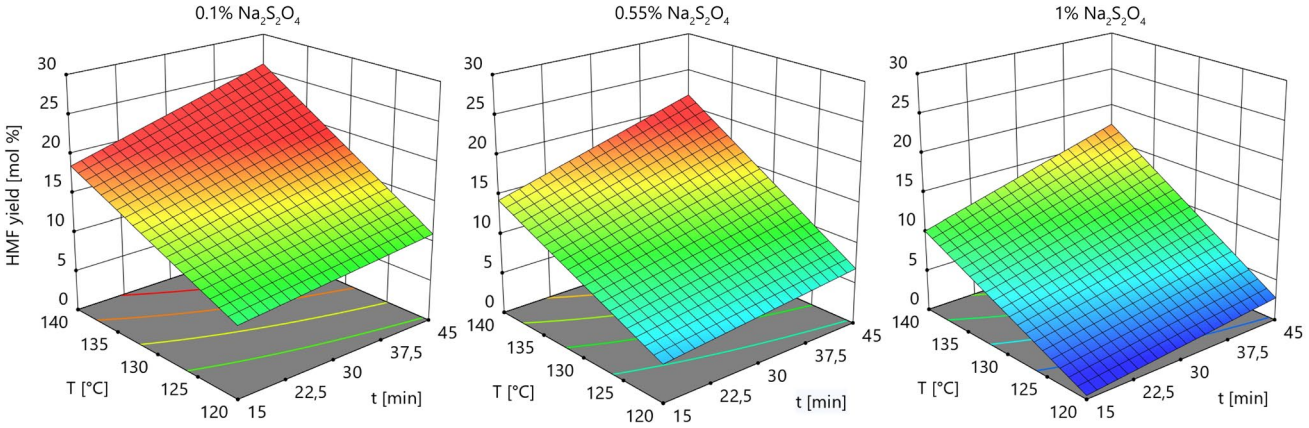

Fig. 5 Influence of the reaction time [min] and the reaction temperature [°C] on the 5-HMF yield [mol%] at different sodium dithionite contents of 0.1, 0.55 and 1 wt%

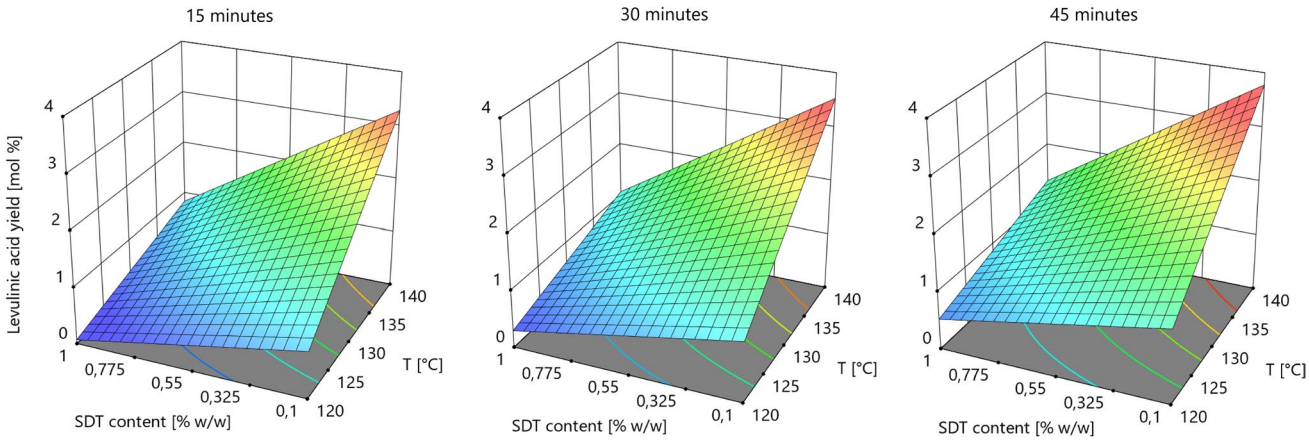

Fig. 6 Influence of the reaction time [min] and the reaction temperature [°C] on the levulinic acid yield [mol %] at different sodium dithionite contents of 0.1, 0.55 and 1 wt%

used stabilizer content. The reaction time was found to have the least impact. All three factors were statistically significant for the 5-HMF and levulinic acid yield models.

For the 5-HMF yield, the developed model showed a good fit for the data, with an $R^2 = 0.9365$, no significant lack of fit and a model p-value of 0.001.

Figure 5 obviously shows that the temperature had a greater influence on the outcome than the reaction time. Sodium dithionite addition generally slows the reaction down and leads to lower yields. Although this is not directly desired for 5-HMF, this drawback is overcompensated by a strong reduction of side product formation. As shown in Fig. 6, the yield of levulinic acid is decreased from a maximum of 4 mol% to < 1.5 mol%. The developed model for levulinic acid formation showed $R^2 = 0.9130$, no significant lack of fit and a model p-value of 0.0025. This indicates that the model is significant and can well be used to predict levulinic acid yields.

Unfortunately, the developed model was not significant for the mass loss (humin mass formed) during the reaction. This is most likely due to the emptying process for the cooling system, which was emptied by blowing pressurized air through the tube. This process was not strictly reproducible and had no defined end point, which makes it likely that it was not always carried out in the exact same way and for the same time. This may have led to incomplete collection of the reaction solution. However, it was evident that the reactions in the presence of 1 wt% of sodium dithionite lead to nearly no humin deposition on the inner reactor surfaces and the mass loss in these reactions remained constant. The deposition of insoluble humins during the reaction run was nearly completely eliminated. Some thin layers of deposits formed eventually during the emptying process on the hot reactor surfaces and could be easily removed.

With this accumulated reaction data, good conditions for the production of the adhesive precursor in this reaction system were identified: 140 °C, 33 min and 1 wt% sodium dithionite. The reaction carried out at these conditions yielded 13.4 mol% 5-HMF (69 g/L). The prognosis (DoE) 15 mol% 5-HMF yield where not reached, which means that the model could be further refined. In an attempt to further improve the reaction conditions, the reactor was pressurized to 0.35 MPa before the heating of the solution to avoid foaming and the stirring speed was raised to 400 rpm. Also, the reaction volume was increased to 1000 g, which is close to the maximum capacity of the reactor (volume of 1 L). After this adjustment, the reaction had a constant yield of 73 ± 3 g/L (n = 6) which corresponds to 5.9 wt% of 5-HMF in the final precursor and a yield of 14.15 mol% 5-HMF. This is already very close to the predicted 15 mol% of the DoE model. On average 980 g of reaction solution were collected in these reaction runs, which corresponds to a mass loss of only 3 wt%, which can be further reduced by optimization of the cooling system.

Although the reaction mechanism of the 5-HMF stabilization by sodium dithionite still remains speculative, the positive effect of sodium dithionite on the reaction system as reported by Gomes et al. [21] was confirmed. The stabilizing impact of the reducing agent on this reaction points either to a possible involvement of oxidation processes during 5-HMF degradation or polymerization, which are impeded, or to a discrimination of follow-up reactions leading to humins and levulinic acid over the targeted formation of 5-HMF from fructose.

3.3 5-HMF-rich precursor stability and utilization

To see whether the precursors produced with the batch reaction system had good storage stability, samples of precursor were stored at room temperature for one week and the 5-HMF concentration was determined again. The concentration of 5-HMF dropped by 0.3 wt% within one week, pointing to condensation of 5-HMF, since levulinic acid levels remained constant. Neutralization of the precursor solution with NaOH reduced the 5-HMF loss to 0.2 wt%. Furthermore, the neutralization of the solution caused dissolution of the small particles, which were present in the acidic precursor. This effect is shown in the microscopic images in Fig. 7. This behavior points to the presence of substances of higher molecular weight (oligomers). It is assumed that these substances contain acidic functions, such as carboxylic acid and phenolic hydroxy moieties, since this would lead to better solubility as the solution gets less acidic (increasing pH). This behavior is well known from polyphenols or some technical lignins, for instance.

The formation of small 5-HMF oligomers should not interfere with later resin synthesis, it might even improve the adhesives' performance. Nevertheless, the stability results suggest that the precursor is not stable for long time periods over weeks and should be used soon after production.

The obtained adhesive precursors were successfully used in adhesive synthesis. The optimization of the synthesis is to be presented in a follow-up publication [23]. The adhesives are produced using bishexamethylene triamine as an additional cross-linker in the fructose/5-HMF system. This leads to structurally very complex adhesive mixtures, since multiple reactions can occur between the cross-linkers, the fructose and the side products of the production process. The scaling process to produce enough precursor for the production of 10 kg of adhesive in a reasonable time frame was successful. The adhesive amount required for one particleboard press series was successfully synthesized with the precursor produced in only three runs in the batch reaction system. Since the reaction

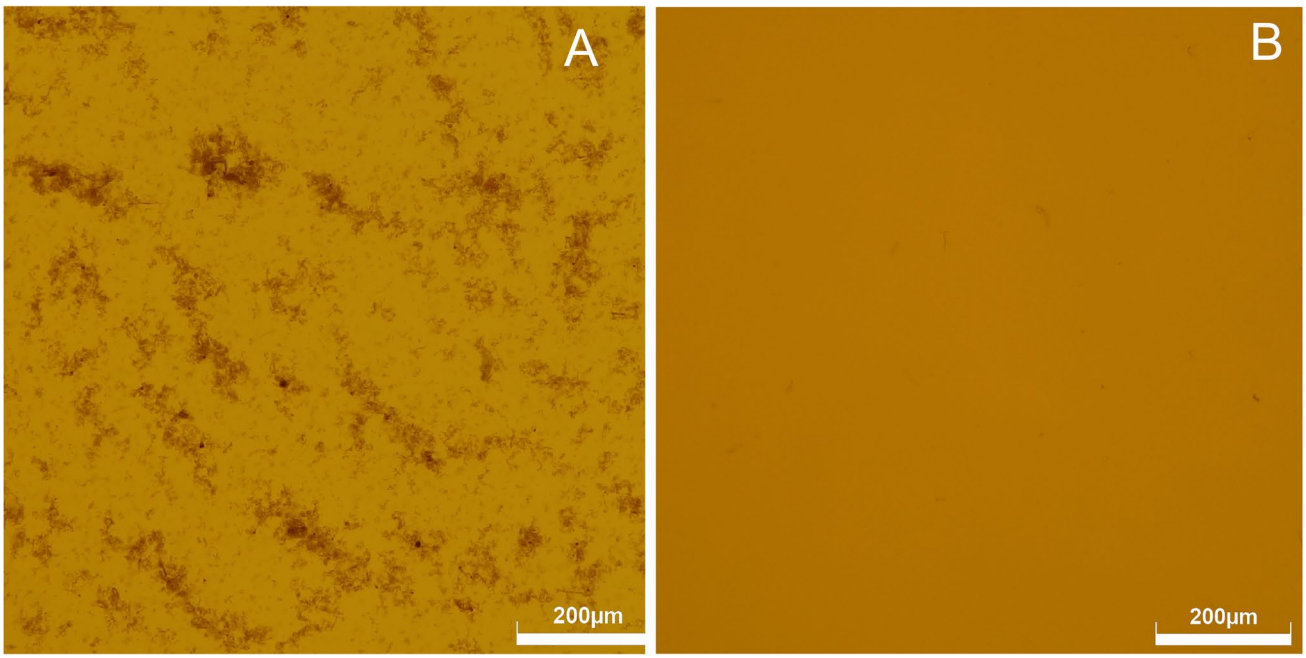

Fig. 7 Micrographs of the acidic (**A**) and neutralized (**B**) precursor solutions

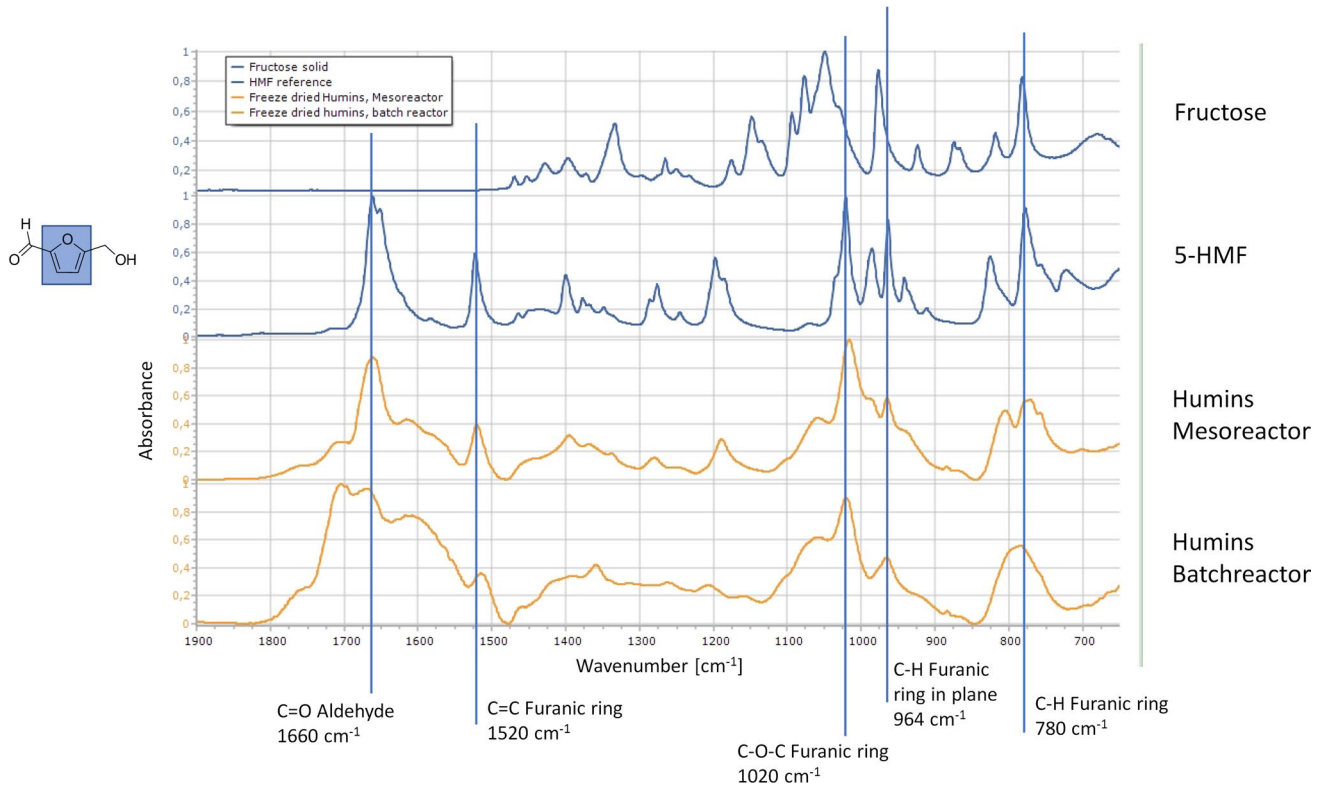

Fig. 8 Overlay of the fingerprint region of the FTIR spectra of fructose, 5-HMF, and two humin samples. Bands from the furan core are indicated by vertical lines

solution is heated to the desired temperature before starting the reaction, the upscaling to industrial scale should be easier for the present system than for alternatives. The pressurized dosing system is realized quite easily also on industrial scale, employing available external pressure sources. In addition, the pressure in the batch reaction is quite moderate, being set to 0.35 MPa and never reaching more than 0.5 MPa during the reaction. These pressures are low in comparison to those in various other industrial processes [24].

Detailed results from the particleboard trials will be discussed in a follow-up publication [25]. Related rheokinetic properties of the produced adhesives have already been discussed [13, 22].

3.4 Analysis of humin side products

FTIR spectra of the humin byproducts from concentrated mesoreactor solution and those from batch precursor production, measured after freeze-drying, are shown in Fig. 8. The spectra of fructose and 5-HMF are listed for comparison. As shown in Fig. 8, the furanic bands at 1521 cm^{-1}, 1020 cm^{-1}, 964 cm^{-1} and 780 cm^{-1} remain present also in the formed humins. This indicates, as also published by Ghatta et al. [16], that the furanic moiety remains stable during the humin formation process or is incorporated as structural units into ladder-type furan-quinoid oligomers as identified by Rosenau et al. [12].

The decrease of the peaks at 1400 cm^{-1} (OH deformation), 1200 cm^{-1} (C–OH) and 720 (CH_2 rocking) points to a polymerization via the -OH moiety of the 5-HMF molecule. These signals are marked in Fig. 9.

Furthermore, similar to observations by Shen et al. [18], the formation of new peaks at 1705 cm^{-1} and 1612 cm^{-1} was observed. Shen et al. assigned these peaks to the C = O and C = C peaks formed by the aldol-like condensation of 5-HMF with levulinic acid (Scheme 2). The original C = O aldehyde peak of 5-HMF is slightly decreased in the formed humins, therefore it is likely that the aldehyde moiety takes part in the reaction, but is not the main reaction side during humin formation. This thesis is also supported by a small band at around 2930 cm^{-1}, which can be assigned to aldehyde C-H bonds found in the humin spectra. Finally, a new band at 1061 cm^{-1}, can be assigned to C–O–C moieties formed during the reaction. This C–O–C band along with the strong absorption around 1600 cm^{-1} argues in favor of intact furanoid systems and/or benzoid moieties being formed. The humins collected from the mesoreactor can be seen as early-stage product, since the band characteristic for humins can already be detected but

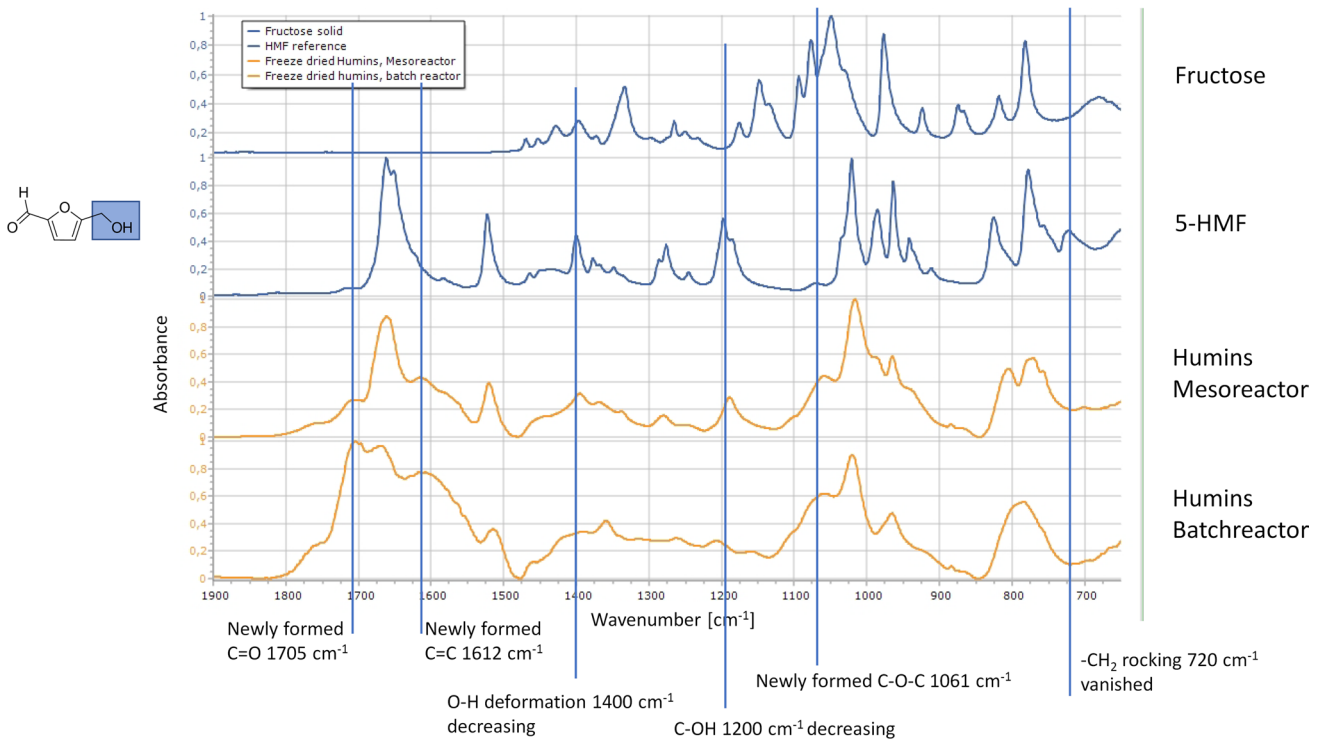

Fig. 9 Overlay of the fingerprint region of the FTIR spectra of fructose, 5-HMF, and two humin samples. Bands from the -CH_2-OH moiety and newly formed bands are indicated by vertical lines

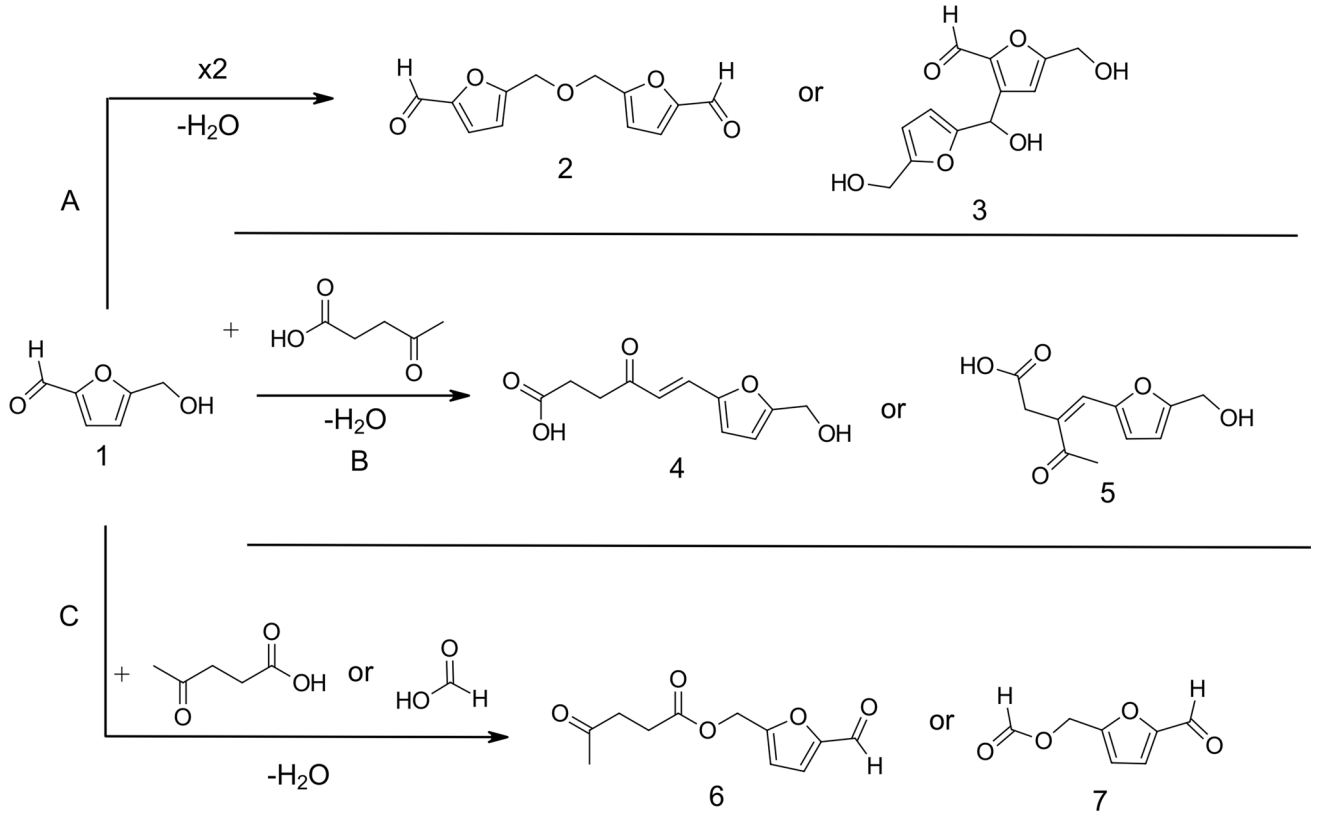

Scheme 2 Proposed initial reactions involving 5-HMF in the humin formation process, (A) etherification or acylation, (B) aldol-type reactions with levulinic acid, (C) esterifications

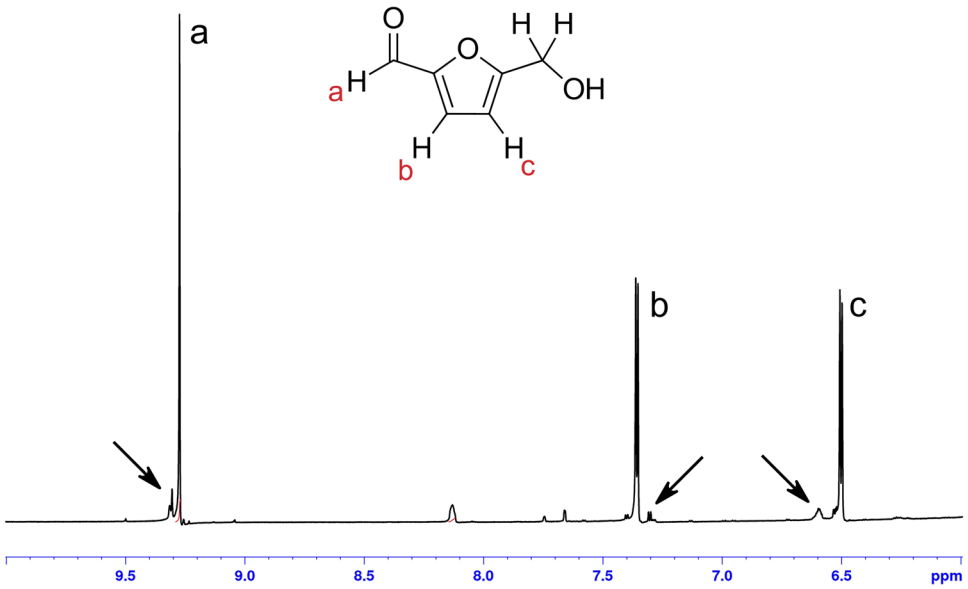

Fig. 10 ^{1}H NMR spectrum of the reaction mixture of a typical conversion from fructose to 5-HMF, region from 6–10 ppm. Peaks of the the 5-HMF dimer (see Scheme 2) are marked with arrows

are not as pronounced as in the spectrum of the humins from the batch reaction system. An overlay of the full FTIR spectra can be found in the supporting information as well as a full ^{1}H NMR spectrum of the products of a typical conversion from fructose to 5-HMF. Figure 10 depicts the region from 6 to 10 ppm of such a ^{1}H NMR spectrum.

The prominent doublets at 6.50 and 7.36 ppm originate from the furan ring hydrogens in 5-HMF, the singlet at

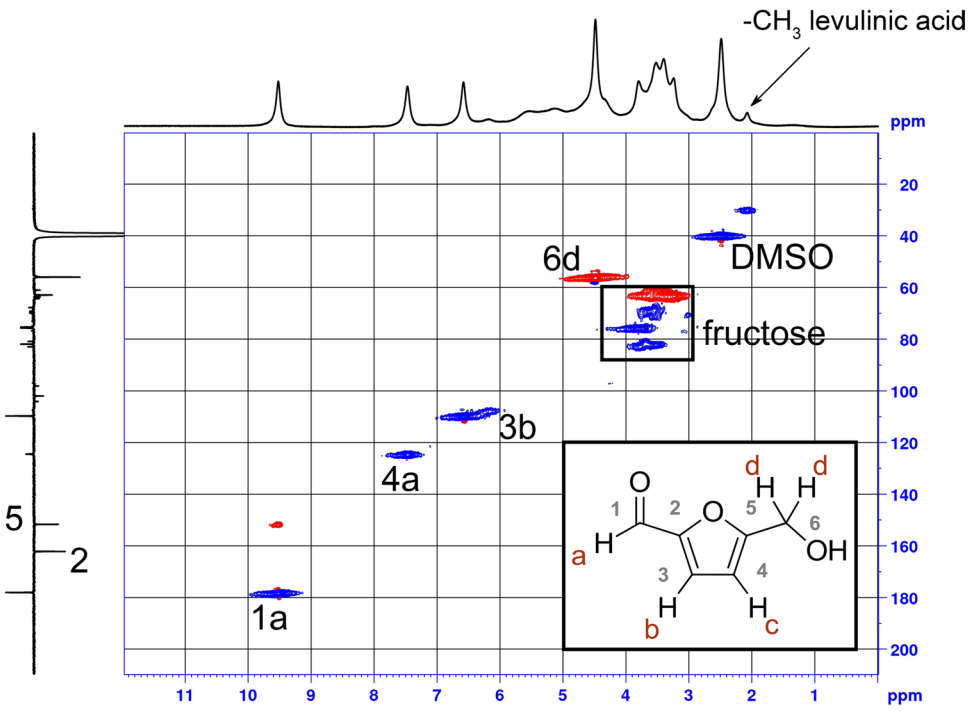

Fig. 11 ^{1}H-^{13}C HSQC spectrum (with peak assignment) of humins produced during the mesoreactor process

9.28 ppm from its aldehyde hydrogen. The small resonances next to the dominant ones, at 6.59, 7.30 and 9.30 ppm and indicated by arrows in Fig. 10, are assigned to the 5-HMF dimer (compound **2** in Scheme 2), which is formed from 5-HMF by etherification. The detection of these peaks and their assignment is in line with reports from Gomes et al. [21] and Shen et al. [18]. The formation of such dimers also agrees with the formation of new C–O–C bands at 1061 cm^{-1} in the FTIR spectra. The small peak at 8.13 ppm originates from formic acid.

The HSQC spectrum of the humin precursors obtained from the mesoreactor solutions (Fig. 11) did not present a lot of new information. All major peaks found could be assigned to either 5-HMF, fructose or levulinic acid, the main components in the reaction solution. On the one hand, this suggests that residual fructose and 5-HMF are

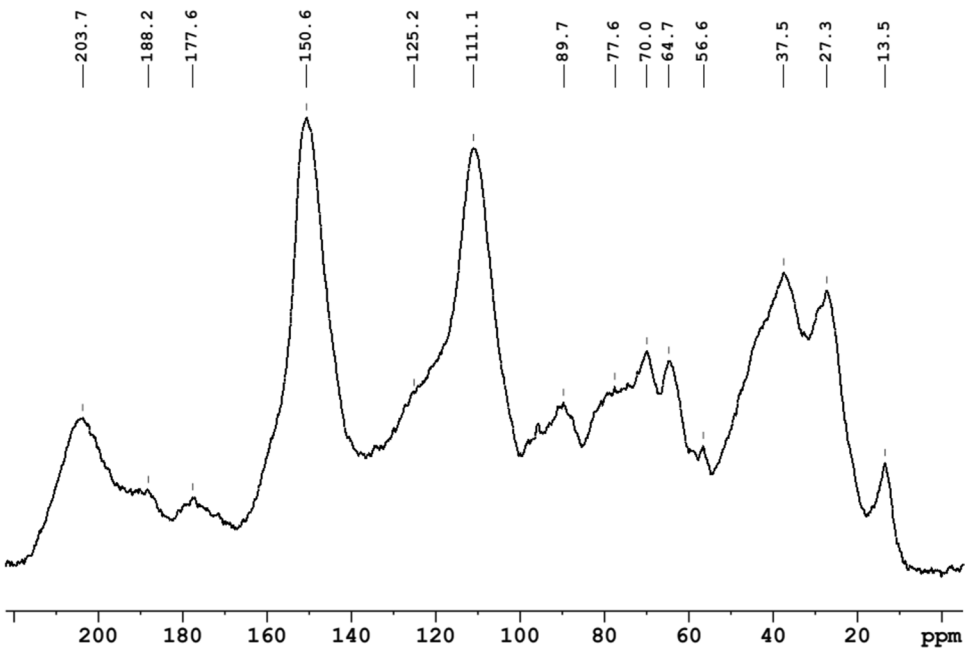

Fig. 12 ^{13}C solid-state NMR of the humins produced in the batch reaction process

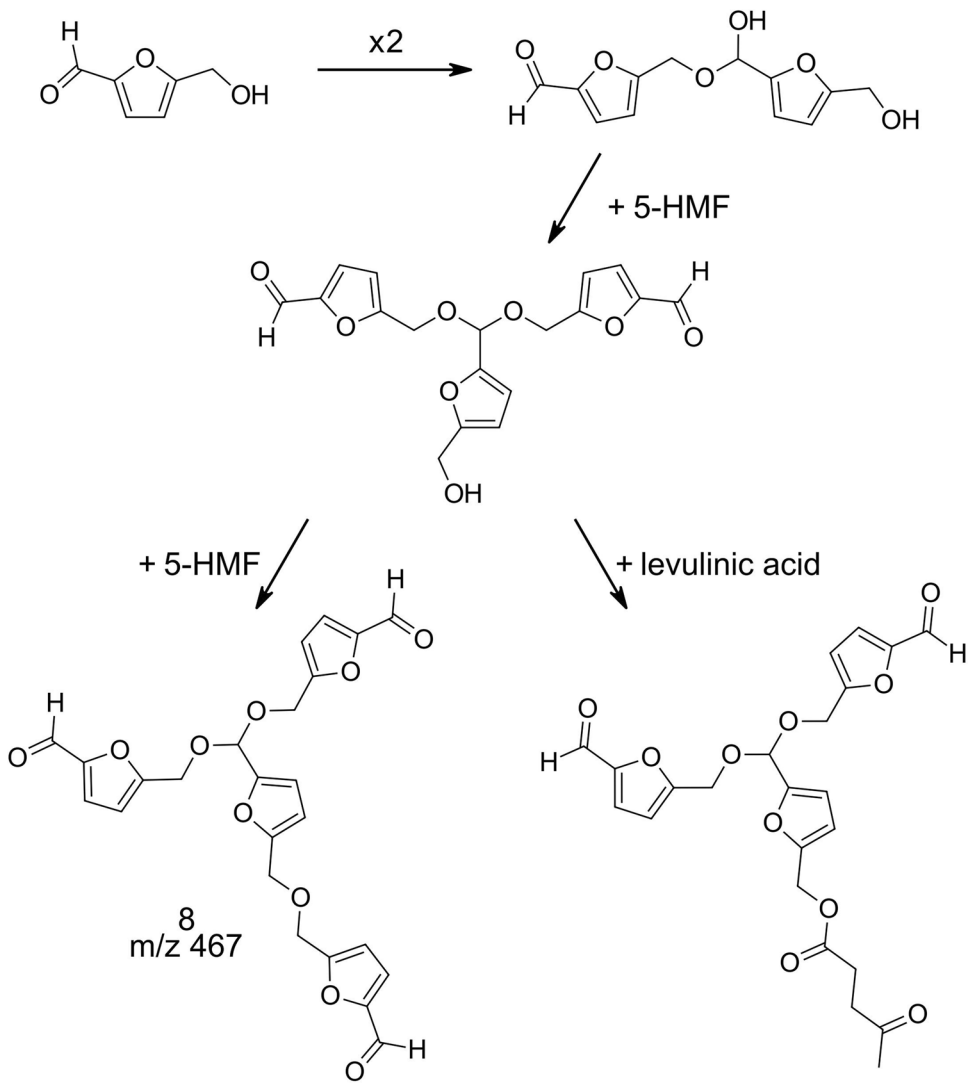

Scheme 3 5-HMF acetal formation as proposed by Shen et al. [18] and al Ghatta et al. [16]

incorporated in the final humin structure by either etherification, strong non-covalent interaction (hydrogen bonding) or also physical entrapment. On the other hand, the proposed ladder-type oligomers as humin-like structures [19] are highly symmetric and possess very few detectable protons which, in addition, can undergo H–D exchange which additionally reduced detectability in ^{1}H NMR. The resonances around 3.5 ppm / 60–80 ppm can be assigned to either fructofuranose or tetrahydrofurane intermediates (rehydrated furans). C1 and C6 of fructofuranose lead to signals at 63 and 64 ppm in the ^{13}C spectrum with corresponding peaks at 3.2 and 4 ppm in the ^{1}H spectrum, C3 and C4 are found at 75.3 and 75.7 ppm and 3.8 ppm, respectively, and C5 at 82 ppm and 3.5 ppm. Resonances were extracted from the HSQC spectrum and assigned according to Kalinowski–Berger–Braun [26].

To gain more information on the structure of humin samples, despite the relative silence of the ^{1}H spectra, a solid-state ^{13}C NMR spectrum was recorded (Fig. 12). Again, the signals of the furanoid structures at around 150 and 110 ppm were very prominent. Also, the resonance around 177 ppm corresponds to the aldehyde carbon in 5-HMF or benzoquinoid (conjugated) keto groups as in the ladder-type oligomers (Scheme 4). Only a weak signal is found for the original hydroxymethyl group of 5-HMF at 56 ppm, again suggesting consumption of this moiety. Peaks at 65 or 70 ppm can be assigned to -CH2-OR moieties as, e.g., in the 5-HMF dimer (compound **2**, Scheme 2). The region of fructofuranose or hydroxylated tetrahydrofurans has relatively low intensity, indicating more complete consumption than in the above-discussed humin precursors from the mesoreactor process. Peaks above 185 ppm point to the formation of new keto functionalities, while the high-field resonances below 40 ppm indicated aliphatic (methylene and methyl) groups, probably originating from levulinic acid products. As already mentioned in the section on FTIR analysis, this incorporation could happen through aldol-type condensation of the 5-HMF aldehyde with levulinic acid as the initiating

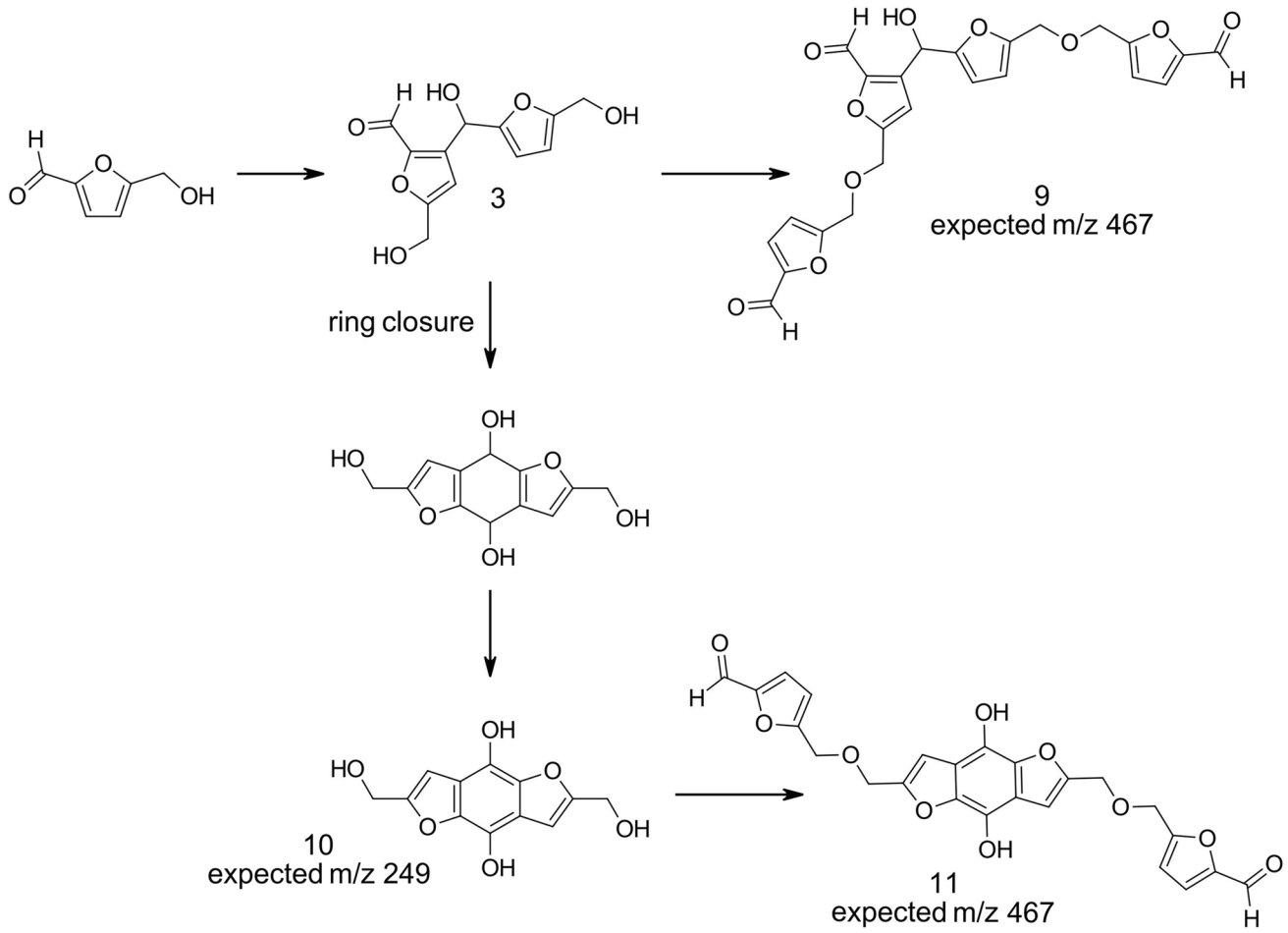

Scheme 4 Chromophores tentatively formed upon humin formation based on MS data

step, as shown in Scheme 2. The formed intermediate (*E*)-6-[5-(hydroxymethyl)furan-2-yl]-hex-4-oxo-5-enoic acid (compound **4** in Scheme 2) has been detected and confirmed by Shen et al. [18] by HPLC–MS and comparison with the authentic compound. Amarasekara et al. [27] synthesized the compound in a base-catalyzed aldol condensation of 5-HMF with levulinic acid, with the reported ^{13}C NMR being in good accordance with those in this work. The region around 125 ppm indicated a C = C double bond as the one in this compound or the quinoid double bonds of oligomers similar to those in Scheme 4. The lower intensity of the signal can be explained by the relatively low abundance of olefinic structures not carrying a hydroxyl or ether moiety (cf. Scheme 4).

Scheme 2 depicts the initial side reactions of 5-HMF that are likely to occur during the humin formation process. Compound **3** was also reported by Badoux et al. [28] in a patent application for the swiss company AVA Biochem, the only industrial 5-HMF producer. Compound **5** was synthesized as alternative aldol condensation product of levulinic acid and 5-HMF by Amarasekara et al. [27] under base catalysis. Compounds **6** and **7**, the levulinate and formiate that are formed by esterification reaction with 5-HMF, were confirmed by Shen et al. [18] by HPLC–MS and comparison with the authentic compounds.

Both Shen et al. and al Ghatta et al. propose the formation of acetals during the reaction (Scheme 3). We consider this formation as highly unlikely under our reaction conditions, since acetals usually are not stable in acidic environment. Similarly, hemiacetals as in furanoses and pyranoses are opened up quickly via oxacarbenium ions and furans undergo complex dehydration/rehydration processes [29]. 5-HMF acetals have even been used by Kirchhecker et al. [30] to enable acidic debonding of polyurethane adhesives.

The depicted tetramer unit (compound **8**, Scheme 3) was proposed based on a peak in the mass spectrum at $m/z = 467$. We propose an alternative structure for this compound (Scheme 4), formed by attack of the protonated aldehyde moiety on the furanic ring of a second 5-HMF molecule and possible subsequent ring closure. This reaction is strongly favored by the acidity of the medium and the furan structure being highly electron-rich. The formation

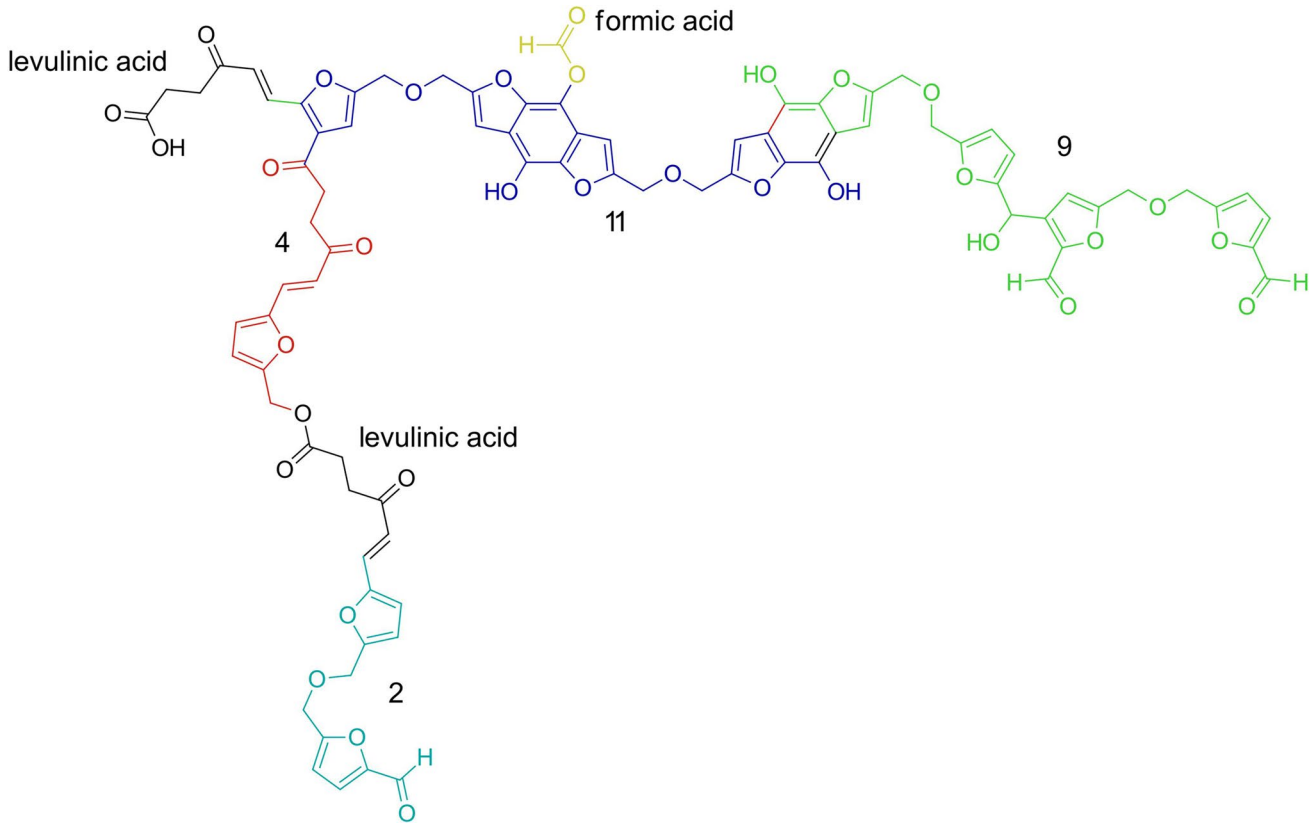

Scheme 5 Structural elements (color coded) in the formed humins: formic acid (yellow), levulinic acid (black) and compounds **2** (gray), **4** (red), **9** (green) and **11** (blue)

of such a ring system explains the strong coloration of the reaction solution, even at low levels of 5-HMF formation, while all structures in Scheme 3 would be colorless in pure form (no conjugation beyond the furan system). Tentative structures of these strong chromophores, which also explain the mass peak of $m/z = 249$ found in the mass spectrum by al Ghatta et al., are shown in Scheme 4. Similar structures were reported by Rosenau et al. in their work on the chromophores from hexeneuronic acids [15]. Their optical electronic structure has been studied by Kumart et al.[31] Although the above indications render it likely that humins are at least to certain extent represented by such structures, conclusive proof for their formation is not provided by the solid-state ^{13}C NMR and IR data.

Taking all this gathered information into account, we propose the formed humins to possess the following structural elements (Scheme 5).

The DSC measurements of the humin samples (Fig. 13) showed that the humins from the batch reactor were stable in the range of 50–300 °C. This is different from the case of the humins formed in the mesoreactor process, which show a clear reaction peak at 167 °C, with a small remaining contribution of the fructose decomposition peak at 218 °C. This supports, as already mentioned above in connection with the FTIR spectra, that the humins from the mesoreactor process can be seen as intermediates of the larger structures formed in the batch process.

4 Conclusion

An adhesive precursor solution based on high-fructose syrup, containing 5-HMF levels suitable for adhesive synthesis, was successfully produced in an adjusted batch reaction system. The reactor was equipped with a pressurized dosing system to allow precise heating times and with a cooling system that eliminates differences in cooling time, which ensured comparability of reactions at different temperatures. Sodium dithionite was successfully used to reduce byproduct formation and the reaction conditions were optimized in a DoE approach, with 140 °C, 33 min reaction time and 1% $Na_2S_2O_4$ content (yielding 73 g/L of HMF) as the outcome. The reaction temperature was found to have the biggest influence on the reaction, followed by the stabilizer content and the reaction time. The precursor needed for the production of 10 kg of adhesive was produced in only three runs in the batch reaction system, which was not

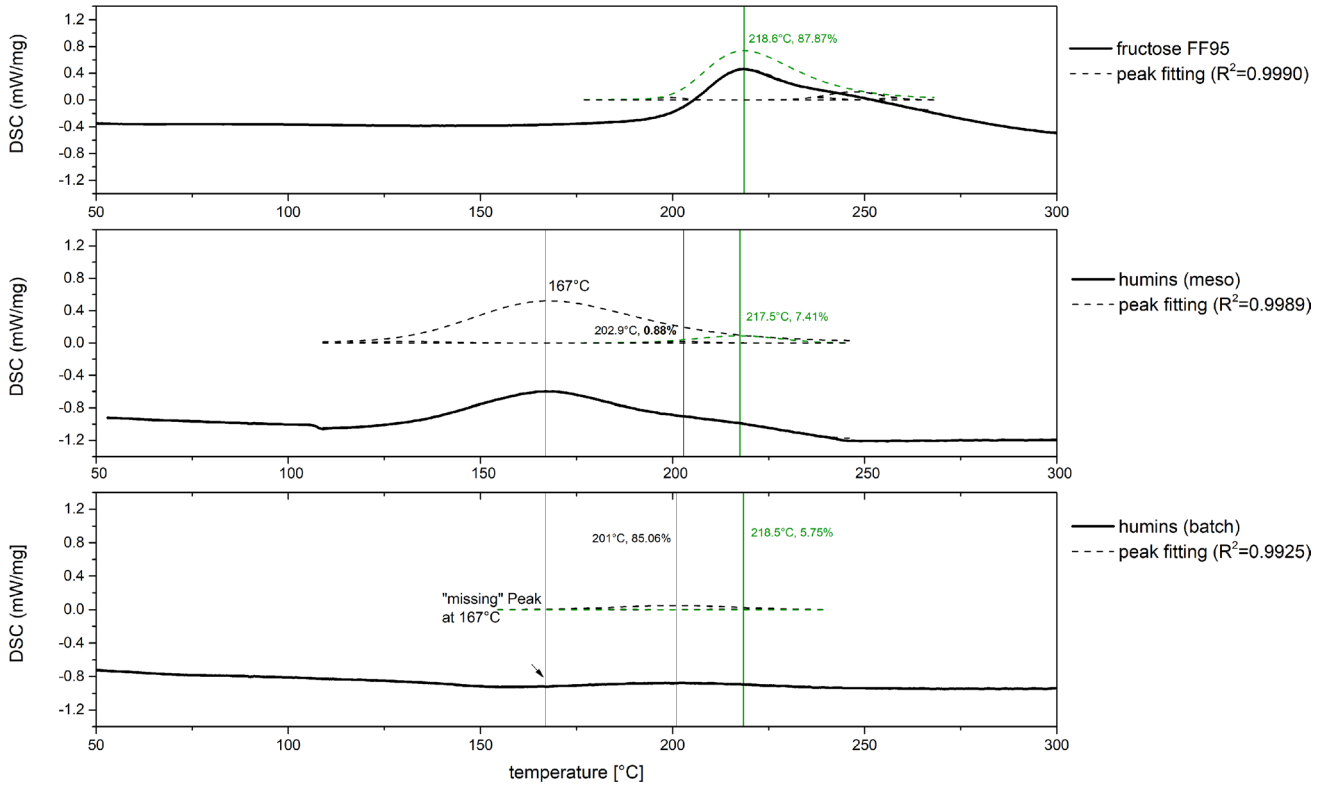

Fig. 13 DSC analysis of humin samples and fructose syrup at 5 °C/min

easily achievable with the continuous reaction system, so that now the testing of the new adhesive systems in particle board trials was possible.

Samples of the major humin byproducts produced during the adhesive precursor synthesis were collected from the batch process and the previous mesoreactor process. These samples were analyzed with NMR and FTIR spectroscopy as well as differential scanning calorimetry, and the gathered data were compared to the available literature on humin structure. With the collected information, possible structural elements of humin matter, in agreement with all available analytical data, were proposed.

Supplementary Information The online version contains supplementary material available at https://doi.org/10.1007/s13399-022-03200-x.

Author contribution **Wilfried Sailer-Kronlachner** was responsible for conceptualization, methodology, investigation, validation, formal analysis, writing the original draft and visualization. **Catherine Rosenfeld** was involved in conceptualization, investigation, validation, formal analysis, writing, review and editing, and visualization. **Stefan Böhmdorfer** contributed to writing, review and editing, visualization, and supervision. **Markus Bacher** took part in investigation, validation, writing, review and editing, and visualization. **Johannes Konnerth**, **Thomas Rosenau** and **Antje Potthast** participated in writing, review and editing, supervision, and resources. **Andreas Geyer** was responsible for writing, review and editing, and resources. **Hendrikus W.G. van Herwijnen** was involved in methodology, writing, review and editing, supervision, resources, project administration and funding acquisition.

Funding Open access funding provided by University of Natural Resources and Life Sciences Vienna (BOKU). This work was carried out in the framework of the European Project SUSBIND. It has received funding from the Bio-based Industries Joint Undertaking (BBI-JU) under grant agreement No. 792063. The BBI-JU receives support from the European Union's Horizon 2020 research and innovation program.

Data availability The datasets generated during and/or analyzed during the current study are not publicly available due to confidentiality issues, but are available from the corresponding author on reasonable request.

Declarations

Conflicts of interest There are no conflicts to declare.

References

1. FAO (2020) FAO Yearbook of Forest Products. FAO - Food and Agric Org United Nations, Rome. https://doi.org/10.4060/cb3795m
2. European-Commission (2014) COMMISSION REGULATION (EU) No 605/2014 of 5 June 2014 amending, for the purposes of introducing hazard and precautionary statements in the Croatian language and its adaptation to technical and scientific progress, Regulation (EC) No 1272/2008 of the European Parliament and of the Council on classification, labelling and packaging of substances and mixtures. OJ L 167/36
3. Röper H (2002) Renewable raw materials in Europe — Industrial utilisation of starch and sugar. Staerke 54(3–4):89–99. https://doi.org/10.1002/1521-379X(200204)54:3/4%3c89::AID-STAR89%3e3.0.CO;2-I
4. Sousa AF, Vilela C, Fonseca AC, Matos M, Freire CSR, Gruter G-JM, Coelho JFJ, Silvestre AJD (2015) Biobased polyesters and other polymers from 2,5-furandicarboxylic acid: a tribute to furan excellency. Polym Chem 6(33):5961–5983. https://doi.org/10.1039/C5PY00686D
5. Liu B, Xu S, Zhang M, Li X, Decarolis D, Liu Y, Wang Y, Gibson EK, Catlow CRA, Yan K (2021) Electrochemical upgrading of biomass-derived 5-hydroxymethylfurfural and furfural over oxygen vacancy-rich NiCoMn-layered double hydroxides nanosheets. Green Chem 23(11):4034–4043. https://doi.org/10.1039/D1GC00901J
6. Rosenfeld C, Konnerth J, Sailer-Kronlachner W, Solt P, Rosenau T, van Herwijnen HWG (2020) Current situation of the challenging scale-up development of hydroxymethylfurfural production. Chemsuschem 13(14):3544–3564. https://doi.org/10.1002/cssc.202000581
7. van Putten R-J, van der Waal JC, de Jong E, Rasrendra CB, Heeres HJ, de Vries JG (2013) Hydroxymethylfurfural, a versatile platform chemical made from renewable resources. Chem Rev 113(3):1499–1597. https://doi.org/10.1021/cr300182k
8. Yu IKM, Tsang DCW (2017) Conversion of biomass to hydroxymethylfurfural: A review of catalytic systems and underlying mechanisms. Bioresource Technol 238:716–732. https://doi.org/10.1016/j.biortech.2017.04.026
9. Hu L, Wu Z, Jiang Y, Wang X, He A, Song J, Xu J, Zhou S, Zhao Y, Xu J (2020) Recent advances in catalytic and autocatalytic production of biomass-derived 5-hydroxymethylfurfural. Renew Sustain Energy Rev 134:110317. https://doi.org/10.1016/j.rser.2020.110317
10. Zhao Y, Lu K, Xu H, Zhu L, Wang S (2021) A critical review of recent advances in the production of furfural and 5-hydroxymethylfurfural from lignocellulosic biomass through homogeneous catalytic hydrothermal conversion. Renew Sustain Energy Rev 139:110706. https://doi.org/10.1016/j.rser.2021.110706
11. Slak J, Pomeroy B, Kostyniuk A, Grilc M, Likozar B (2022) A review of bio-refining process intensification in catalytic conversion reactions, separations and purifications of hydroxymethylfurfural (HMF) and furfural. Chem Eng J 429:132325. https://doi.org/10.1016/j.cej.2021.132325
12. Šivec R, Grilc M, Huš M, Likozar B (2019) Multiscale Modeling of (Hemi)cellulose Hydrolysis and Cascade Hydrotreatment of 5-Hydroxymethylfurfural, Furfural, and Levulinic Acid. Ind Eng Chem Res 58(35):16018–16032. https://doi.org/10.1021/acs.iecr.9b00898
13. Sailer-Kronlachner W, Thoma C, Böhmdorfer S, Bacher M, Konnerth J, Rosenau T, Potthast A, Solt P, van Herwijnen HWG (2021) Sulfuric acid-catalyzed dehydratization of carbohydrates for the production of adhesive precursors. ACS Omega 6(25):16641–16648. https://doi.org/10.1021/acsomega.1c02075
14. König B, Dubnack K (2010) Mikroreaktionstechnik in der Organischen Synthese. Deutsche Bundesstiftung Umwelt (DBU), Osnabrück
15. Rosenau T, Potthast A, Zwirchmayr NS, Hettegger H, Plasser F, Hosoya T, Bacher M, Krainz K, Dietz T (2017) Chromophores from hexeneuronic acids: Identification of HexA-derived chromophores. Cellulose 24(9):3671–3687. https://doi.org/10.1007/s10570-017-1397-4
16. Al Ghatta A, Zhou X, Casarano G, Wilton-Ely JDET, Hallett JP (2021) Characterization and valorization of humins produced by HMF degradation in ionic liquids: A valuable carbonaceous material for antimony removal. ACS Sustain Chem Eng 9(5):2212–2223. https://doi.org/10.1021/acssuschemeng.0c07963
17. van Zandvoort I, Wang Y, Rasrendra CB, van Eck ERH, Bruijnincx PCA, Heeres HJ, Weckhuysen BM (2013) Formation, molecular structure, and morphology of humins in biomass conversion: Influence of feedstock and processing conditions. Chemsuschem 6(9):1745–1758. https://doi.org/10.1002/cssc.201300332
18. Shen H, Shan H, Liu L (2020) Evolution process and controlled synthesis of humins with 5-Hydroxymethylfurfural (HMF) as model molecule. Chemsuschem 13(3):513–519. https://doi.org/10.1002/cssc.201902799
19. Rosenau T, Potthast A, Zwirchmayr NS, Hosoya T, Hettegger H, Bacher M, Krainz K, Yoneda Y, Dietz T (2017) Chromophores from hexeneuronic acids (HexA): synthesis of model compounds and primary degradation intermediates. Cellulose 24(9):3703–3723. https://doi.org/10.1007/s10570-017-1396-5
20. https://susbind.eu/about-susbind-project/public-deliverables/. Accessed 05.07.2022
21. Gomes RFA, Mitrev YN, Simeonov SP, Afonso CAM (2018) Going beyond the limits of the biorenewable platform: Sodium dithionite-promoted stabilization of 5-Hydroxymethylfurfural. Chemsuschem 11(10):1612–1616. https://doi.org/10.1002/cssc.201800297
22. Thoma C, Solt-Rindler P, Sailer-Kronlachner W, Rosenau T, Potthast A, Konnerth J, Pellis A, van Herwijnen HWG (2021) Carbohydrate-hydroxymethylfurfural-amine adhesives: Chemorheological analysis and rheokinetic study. Polymer 231:124128. https://doi.org/10.1016/j.polymer.2021.124128
23. Sailer-Kronlachner W, Rosenfeld C, Konnerth J, van Herwijnen H Influence of critical synthesis parameters and precursor stabilization on the development of adhesive strength in fructose-HMF-amine adhesives. Forest Products Journal, accepted
24. Eggers R (2012) Industrial High Pressure Applications: Processes. Wiley-VCH Verlag GmbH & Co. KGaA, Equipment and Safety. https://doi.org/10.1002/9783527652655
25. Rosenfeld C, Sailer-Kronlachner W, Konnerth J, Solt-Rindler P, Pellis A, Rosenau T, Potthast A, Van Herwijnen HWG (2022) Hydroxymethylfurfural: A key to increased reactivity and performance of fructose-based adhesives for particleboards, under review
26. Kalinowski H-O, Berger S, Braun S (2000) ^{13}C NMR Spektroskopie. Georg Thieme Verlag KG, Wahlstedt
27. Amarasekara AS, Singh TB, Larkin E, Hasan MA, Fan H-J (2015) NaOH catalyzed condensation reactions between levulinic acid and biomass derived furan-aldehydes in water. Ind Crops Prod 65:546–549. https://doi.org/10.1016/j.indcrop.2014.10.005

28. Badoux F, Koehler S, Mortato M, Krawielitzki S (2018) HMF OLIGOMERS. United States Patent 20180244823, 30.08.2018
29. Hosoya T, Takano T, Kosma P, Rosenau T (2014) Theoretical Foundation for the Presence of Oxacarbenium Ions in Chemical Glycoside Synthesis. J Org Chem 79(17):7889–7894. https://doi.org/10.1021/jo501012s
30. Kirchhecker S, Dell'Acqua A, Angenvoort A, Spannenberg A, Ito K, Tin S, Taden A, de Vries JG (2021) HMF–glycerol acetals as additives for the debonding of polyurethane adhesives. Green Chem 23(2):957–965. https://doi.org/10.1039/D0GC04093B
31. Kumar A, Cappellini G, Delogu F (2019) Electronic and optical properties of chromophores from hexeneuronic acids. Cellulose 26(3):1489–1501. https://doi.org/10.1007/s10570-018-2174-8